Extracting current-induced spins: spin boundary conditions at narrow Hall contacts

2007 New J. Phys. 9 382

(http://iopscience.iop.org/1367-2630/9/10/382)

New Journal of Physics
The open–access journal for physics

Extracting current-induced spins: spin boundary conditions at narrow Hall contacts

İ Adagideli[1,3], M Scheid[1], M Wimmer[1], G E W Bauer[2] and K Richter[1]

[1] Institut für Theoretische Physik, Universität Regensburg, D-93040, Germany
[2] Kavli Institute of Nanoscience, TU Delft, Lorentzweg 1, 2628 CJ Delft, The Netherlands
E-mail: inanc.adagideli@physik.uni-regensburg.de

New Journal of Physics **9** (2007) 382
Received 30 July 2007
Published 24 October 2007
Online at http://www.njp.org/
doi:10.1088/1367-2630/9/10/382

Abstract. We consider the possibility to extract spins that are generated by an electric current in a two-dimensional electron gas with Rashba–Dresselhaus spin–orbit interaction (R2DEG) in the Hall geometry. To this end, we discuss boundary conditions for the spin accumulations between a spin–orbit (SO) coupled region and a contact without SO coupling, i.e. a normal two-dimensional electron gas (2DEG). We demonstrate that in contrast to contacts that extend along the whole sample, a spin accumulation can diffuse into the normal region through finite contacts and be detected by e.g. ferromagnets. For an impedance-matched narrow contact the spin accumulation in the 2DEG is equal to the current induced spin accumulation in the bulk of R2DEG up to a geometry-dependent numerical factor.

[3] Author to whom any correspondence should be addressed.

PII: S1367-2630(07)56208-7

Contents

1. Introduction

In recent years, there has been an increasing impetus towards generating and detecting spin accumulations and spin currents in nonmagnetic systems [1]. Recently, as an alternative to spin injection with ferromagnets, spin generation based on two related effects, current-induced spin accumulation (CISA) [2]–[5] and current-induced transverse spin current [6, 7][4] (known as the spin Hall effect (SHE)), has attracted considerable attention. In [6], the SHE was caused by the spin–orbit (SO) interaction of impurities and the effect is then called 'extrinsic'. The 'intrinsic' SHE caused by a band structure with SO-induced spin splitting was proposed by Sinova *et al* [9] for the two-dimensional electron gas with finite Rashba type SO coupling (R2DEG) and Murakami *et al* [10] for the hole gas in bulk III–V semiconductors with significant SO interaction. After an initial controversy, it is now generally agreed that in the diffuse regime the intrinsic spin Hall conductivity vanishes in the bulk of a R2DEG [11]–[14], but remains finite in hole systems, and near the edges of a finite diffusive R2DEG [12, 15]. CISA and the SHE have been observed in semiconductors by optical detection of local spin accumulations [5, 16, 17]. The SHE has also been observed in metals using ferromagnetic leads [18]. Although initial theoretical work on the SHE and CISA have been on bulk disordered conductors [7]–[13], [15, 19, 20], it is now understood that the bulk conductivity is not necessarily related to experimentally relevant quantities such as local spin accumulations probed by local optical or electrical probes. In this respect, a more local approach based on spin diffusion equations is advantageous [12, 13]. However, spin diffusion equations have to be supplemented by suitable boundary conditions that have observable consequences. There have been many proposals in that direction [15], [21]–[26][5], but a consensus has not been reached so far.

Here, we focus on the boundary conditions between a (half infinite) two-dimensional electron gas with SO coupling (R2DEG) and a (half infinite) two-dimensional electron gas (2DEG) without SO coupling connected by a contact that is narrow on the scale of the system, but wider than the mean free path. Such a boundary has been considered [23, 26], but for an

[4] See also [8].
[5] See also [27].

infinitely wide contact region, for which it could be shown that no spin accumulation could diffuse into the 2DEG [26]. We shall show below, however, that for a narrow (as opposed to wide) contact, the spin accumulation in the 2DEG is equal to the bulk value of the spin accumulation in R2DEG up to a numerical constant which depends on the geometry that is smaller than but can be of the order of unity. These results prove that CISA *can* be extracted to a region with small SO coupling in which the spin lifetime is very long and used for spintronics applications, thus confirming our previous results [15].

This paper is organized as follows: we define our model and derive spin diffusion equations in section 2. In section 3, we first recapitulate the symmetry relations for conductances with respect to measuring the spin accumulation in a normal region with ferromagnetic leads. Next, we apply these relations to demonstrate that CISA from the R2DEG can be extracted into a 2DEG region. In section 4, we focus on a model for a small contact between the R2DEG and the 2DEG and solve it to demonstrate the principle of spin extraction to a region with vanishing SO interaction. The numerical simulations for the diffuse R2DEG–2DEG heterostructure are reported in section 5.

2. Spin diffusion equations in a 2DEG with Rashba spin–orbit coupling

In this paper, we focus on a disordered finite size 2DEG with Rashba type SO coupling, noting that the effects of a significant Dresselhaus term can be included straightforwardly. Throughout the paper, we shall assume that all length scales of this finite region are much larger than the elastic mean free path such that spin transport is governed by diffusion equations [12, 13]. In this section, we proceed to derive these spin diffusion equations for later convenience.

In 2×2 spin space, our system is defined by the Hamiltonian:

$$H = \frac{\mathbf{p}^2}{2m} + \alpha \mathbf{p} \cdot (\boldsymbol{\sigma} \times \boldsymbol{z}) + U(\mathbf{x}) + V(\mathbf{x}), \tag{1}$$

where $\mathbf{x}$ and $\mathbf{p}$ are the (two-dimensional (2D)) position and momentum operators, respectively, $\boldsymbol{\sigma}$ is the vector of Pauli spin matrices (the $2\times$ 2 unit matrix is implied with scalars), $\boldsymbol{z}$ is the unit vector normal to the 2D plane, α parameterizes the strength of the SO interaction that can be position dependent, e.g. due to local external gates, $V(\mathbf{x}) = \sum_{i=1}^{N} \phi(\mathbf{x} - \boldsymbol{X}_i)$ is the impurity potential, modeled by N impurity centers located at points $\{\boldsymbol{X}_i\}$, which for the sake of simplicity we assume to be spherically symmetric, and $U(\mathbf{x})$ is a smooth potential that confines the system to a finite region but allows a few openings to reservoirs.

2.1. Rashba Green function

Our starting point is the impurity averaged Green's function $G(k) = (\hbar^2 k^2/2m + \hbar\alpha\boldsymbol{\eta}\cdot\mathbf{k} - E - \mathrm{i}\hbar/\tau)^{-1}$, where $\boldsymbol{\eta} = \boldsymbol{z} \times \boldsymbol{\sigma}$, and τ is the momentum lifetime. In terms of its components, $G(k)$ is given by

$$\frac{\hbar^2}{2m} G(\mathbf{k}) = \frac{1}{2}\left(\frac{1}{k^2 - k_+^2} + \frac{1}{k^2 - k_-^2}\right) + \frac{k_\alpha \mathbf{k}\cdot\boldsymbol{\eta} - k_\alpha^2/2}{k_+^2 - k_-^2}\left(\frac{1}{k^2 - k_+^2} - \frac{1}{k^2 - k_-^2}\right), \tag{2}$$

where $k_\pm^2 = k_F^2 + k_\alpha^2/2 \pm k_\alpha\sqrt{k_F^2 + k_\alpha^2/4} + 2mi/(\tau\hbar)$, $k_\alpha = 2m\alpha/\hbar$ and $k_F = \sqrt{2mE_F/\hbar^2}$. The real space Green function is then obtained by a Fourier transform:

$$G(\mathbf{x}, E_F) = \frac{im}{2\hbar^2}\Bigg[-\frac{1}{2}(H_0^{(1)}(k_+x) + H_0^{(1)}(k_-x)) - \frac{k_\alpha^2/2}{k_+^2 - k_-^2}(H_0^{(1)}(k_+x) - H_0^{(1)}(k_-x)) + \frac{i\boldsymbol{\eta}\cdot\hat{\mathbf{x}}k_\alpha}{k_+^2 - k_-^2}(k_+H_1^{(1)}(k_+x) - k_-H_1^{(1)}(k_-x))\Bigg], \tag{3}$$

where $x = |\mathbf{x}|$ and $H_n^{(1)}$ is the Hankel function of the first kind. We note that we only need the large $k_F x$ asymptotics of $G(x)$, because we are interested in dilute disorder. The conventional approximation [28] is to expand $G(x)$ to leading order in $1/(k_F r)$ and k_α/k_F:

$$G(\mathbf{x}, E_F) \approx -\frac{im}{2\hbar^2}\sqrt{\frac{2}{k_F x}}e^{ik_F x - i\pi/4 - x/2l}e^{-ik_\alpha \mathbf{x}\cdot\boldsymbol{\eta}/2}, \tag{4}$$

where $l = \hbar k_F \tau/m$. This level of approximation is sufficient for most SO related applications such as the calculation of Dyakonov–Perel spin relaxation, spin precession, weak antilocalization etc. However, in order to study CISA and SHE in diffusive systems, it is necessary to go to higher order in $m\alpha/\hbar k_F$ and $1/(k_F x)$. With these correction terms, the asymptotic Green function becomes:

$$G(\mathbf{x}, E_F) \approx \frac{-im}{2\hbar^2}\sqrt{\frac{2}{k_F x}}e^{ik_F x - i\pi/4 - x/2l}\Bigg[e^{-ik_\alpha \mathbf{x}\cdot\boldsymbol{\eta}/2}\left(1 - \frac{k_\alpha}{4k_F}\hat{\mathbf{x}}\cdot\boldsymbol{\eta}\right) - \frac{3i}{8k_F x}e^{ik_\alpha \mathbf{x}\cdot\boldsymbol{\eta}/2} + \frac{i}{8k_F x}\left(e^{ik_\alpha x/2} + e^{-ik_\alpha x/2}\right)\Bigg], \tag{5}$$

where $\hat{\mathbf{x}} = \mathbf{x}/x$. In the next subsection, we will use this expression to derive spin diffusion equations for a R2DEG.

2.2. Diffusion equation

We first focus on the equation of motion of the density matrix with coherent spin components. It can be shown that in the limit $E_F\tau/\hbar \gg 1$, the energy resolved density matrix satisfies the following equation [12, 13, 23, 24]:

$$\rho_a(\mathbf{x}, \omega) = \frac{1}{2\pi\nu\tau}\int d^2x' \mathcal{K}_{ac}(\mathbf{x}, \mathbf{x}'; \omega)\rho_c(\mathbf{x}', \omega), \tag{6}$$

where $\rho_a = \mathrm{Tr}(\rho\sigma_a)$, summation over repeated indices is implied, and ν is the density of states and

$$\mathcal{K}_{ab}(\mathbf{x}, \mathbf{x}'; \omega) = \tfrac{1}{2}\mathrm{Tr}\Big(\sigma_a G^R(\mathbf{x}, \mathbf{x}'; E + \omega)\sigma_b G^A(\mathbf{x}', \mathbf{x}; E)\Big). \tag{7}$$

Multiplying $\rho(E)$ with the density of states and integrating over energy, we obtain the densities and polarizations, whereas accumulations are obtained by directly integrating over energy. The diffusion equation is obtained by expanding equation (7) to second order in spatial gradients. In a homogeneously disordered system we have:

$$\begin{aligned}\rho_a(\mathbf{x}) &= \frac{1}{2\pi\nu\tau}\int d^2r \mathcal{K}_{ac}(\mathbf{r})\rho_c(\mathbf{r} + \mathbf{x}),\\ &\approx \frac{1}{2\pi\nu\tau}\int d^2r \mathcal{K}_{ac}(\mathbf{r})(\rho_c(\mathbf{x}) + \mathbf{r}\cdot\nabla\rho_c(\mathbf{x}) + r_i r_j \partial_i\partial_j\rho_c(\mathbf{x}),\end{aligned} \tag{8}$$

where $\rho_a(\mathbf{x}) = \rho_a(\mathbf{x}; 0)$. We now use the asymptotic expression equation (5) for the Green's function and insert the resulting expression into equation (8). The spatial integrals are elementary and lead to the following equations for the vector components of the density matrix, $\mathbf{s} = (\rho_1/2, \rho_2/2)$, $s_3 = \rho_3/2$ and $n = \rho_0$:

$$D\nabla^2 n - 4K_{\mathrm{s-c}}(\nabla \times \mathbf{s})_z = 0, \tag{9}$$

$$D\nabla^2 s_3 - 2K_{\mathrm{p}}(\nabla \cdot \mathbf{s}) = \frac{2s_3}{\tau_{\mathrm{s}}}, \tag{10}$$

$$D\nabla^2 \mathbf{s} + 2K_{\mathrm{p}}\nabla s_3 - K_{\mathrm{s-c}}(\mathbf{z} \times \nabla)n = \frac{\mathbf{s}}{\tau_{\mathrm{s}}}, \tag{11}$$

here $D = v_{\mathrm{F}}^2\tau/2$, $\tau_{\mathrm{s}} = \tau(1+4\xi^2)/2\xi^2$ (the Dyakonov–Perel spin relaxation time), $K_{\mathrm{s-c}} = \alpha\xi^2/(1+4\xi^2)$, $K_{\mathrm{p}} = \hbar k_{\mathrm{F}}\xi/m(1+4\xi^2)^2$ and $\xi = \alpha p_{\mathrm{F}}\tau/\hbar$. A similar expansion for the spin current, this time to first order in the spatial gradients, produces the analog of Fick's law for spin diffusion:

$$j_j^i = \frac{\nu v_{\mathrm{F}}\xi}{1+4\xi^2}\left(\delta_{i3}\left(s_j - \epsilon_{jm3}\frac{\alpha\tau}{2}\nabla_m n\right) - \delta_{ij}s_3\right) - \nu D\nabla_j s_i. \tag{12}$$

When supplied with suitable boundary conditions the diffusion equations (9)–(11) and the spin current expression (12) can be solved to obtain all spin and charge conductances. Here, we are mainly interested in the boundary between a R2DEG and a 2DEG (for hard wall boundary conditions see [21, 23, 24]). In this case, the boundary conditions require the continuity of the spin current [15, 26]

$$\frac{\nu v_{\mathrm{F}}\xi}{1+4\xi^2}\left(\delta_{i3}\left(\mathbf{n}\cdot\mathbf{s}^{\mathrm{R}} - \frac{\alpha\tau}{2}\mathbf{z}\cdot(\mathbf{n}\times\nabla)n\right) - n_i s_3^{\mathrm{R}}\right)\Big|_0 - \nu D\mathbf{n}\cdot\nabla s_i^{\mathrm{R}}.\Big|_0 = \nu D\mathbf{n}\cdot\nabla s_i^{\mathrm{N}}\Big|_0, \tag{13}$$

where $\mathbf{s}^{\mathrm{R}}$ and $\mathbf{s}^{\mathrm{N}}$ are the spin accumulations in the R2DEG and the 2DEG, respectively, and $\mathbf{n}$ is the unit normal vector at the interface. A common choice for the matching condition for the spin accumulation at the interface is to assume that the spin accumulations are continuous (see e.g. [1]):

$$\mathbf{s}^{\mathrm{R}}\Big|_0 = \mathbf{s}^{\mathrm{N}}\Big|_0. \tag{14}$$

This condition has been criticized recently in [26] in which it was demonstrated that for an infinite interface with a constant electric field parallel to it:

$$\left(\mathbf{s}^{\mathrm{R}} + \frac{\alpha\tau}{2}\mathbf{n}\Big(\mathbf{n}\cdot(\mathbf{z}\times\nabla n)\Big)\right)\Big|_0 = \mathbf{s}^{\mathrm{N}}\Big|_0. \tag{15}$$

We first note that when the charge current is perpendicular to the interface, such as for a two-probe configuration[6], these two boundary conditions agree and no controversy exists. However, for an infinite interface where the charge current density is homogeneous, the difference between these two boundary conditions is drastic: if equation (14) is valid, a CISA diffuses into the 2DEG. On the other hand, if equation (15) is valid, the spin accumulation vanishes in the 2DEG. We solve this conundrum below by showing that for a contact smaller than the spin relaxation length (as assumed in [15]), the two boundary conditions lead to results that agree up to a numerical factor of the order of unity. We therefore conclude that it *is* possible to extract spin accumulation to the 2DEG and detect it with a ferromagnet.

[6] Note however that in the two-probe set-up, current induced spin accumulation in R2DEG does not generate an electrical signal up to order $\alpha^2/v_{\mathrm{F}}^2$ [29].

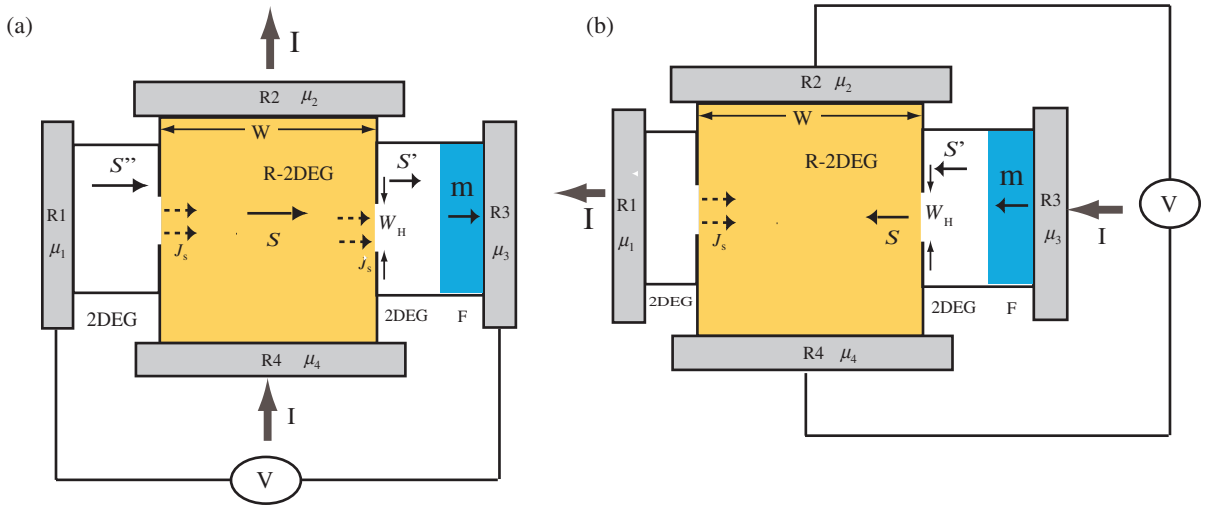

Figure 1. Set-up for detection of current induced spins.

3. Onsager's relations and the spin boundary conditions

In this section, we provide a general symmetry argument based on Onsager's relations, that proves viability of electric detection of the SHE and the CISA by finite size contacts. Let us start by addressing the symmetry properties of multiprobe conductances relevant for the combination of a SO coupled region with a ferromagnet via a normal region (figure 1), using Onsager's relations [29]–[33]. We are particularly interested in the set-up shown in figure 1. The configuration in figure 1(a) is designed to measure the spin accumulation in the 2DEG injected from the neighbouring R2DEG. The voltage signal V directly observes boundary conditions between R2DEG and 2DEG when the charge current is *parallel* to the boundary. The set-up in figure 1(b), on the other hand, measures how much spin is injected into the R2DEG from the ferromagnet through the 2DEG. Then V measures directly the spin boundary conditions for a charge current *perpendicular* to the boundary. Onsager relations relate these two conductances, enabling us to relate the boundary conditions when the current is parallel or perpendicular to the boundary.

3.1. Onsager's relations

In this subsection, we focus on the specific four-probe set-up in figure 2 (for a more general discussion of Onsager's relations in the present context we refer to [29]). The currents in the leads and the respective chemical potentials of the reservoirs are related in linear response as $I_i = \sum_j G_{ij}\mu_j$. We now use the Landauer–Büttiker formalism to obtain G_{ij}. The scattering matrix for the SO coupled region and the ferromagnetic region is given respectively by $S_{\rm SO}$ and $S_{\mathbf{m}}$. The symmetry properties of these matrices are self-duality (reflecting the presence of SO coupling) $S_{\rm SO} = \Sigma_2 S_{\rm SO}^{\rm T} \Sigma_2$, and $S_{\mathbf{m}} = \Sigma_2 S_{-\mathbf{m}}^{\rm T} \Sigma_2$, where Σ_2 is block diagonal in the Pauli matrix σ_y [34]. We are interested in the block structure of $S_{\rm SO}$ singling out lead 5 combining the SO and F regions:

$$S_{\rm SO} = \begin{pmatrix} r_{\rm SO} & t'_{\rm SO} \\ t_{\rm SO} & r'_{\rm SO} \end{pmatrix}, \tag{16}$$

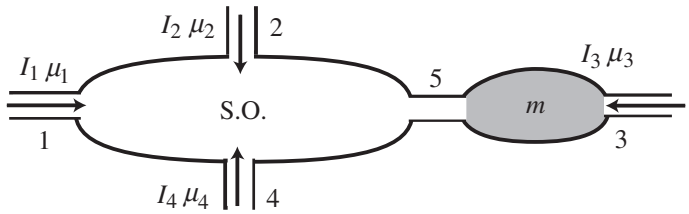

Figure 2. A generic four-probe set-up for the detection of current-induced spins.

where the matrix r_{SO} includes all reflections and transmissions that begin and end in the leads 1, 2 and 4. Using the rules for combining S-matrices, we obtain the joint S-matrix of the combined SO|F region:

$$t = t_{\mathbf{m}}[1 - r'_{\mathrm{SO}} r_{\mathbf{m}}]^{-1} t_{\mathrm{SO}}, \tag{17}$$

$$t' = t'_{\mathrm{SO}}[1 - r_{\mathbf{m}} r'_{\mathrm{SO}}]^{-1} t'_{\mathbf{m}}, \tag{18}$$

$$r = r_{\mathrm{SO}} + t'_{\mathrm{SO}} r_{\mathbf{m}}[1 - r'_{\mathrm{SO}} r_{\mathbf{m}}]^{-1} t_{\mathrm{SO}}, \tag{19}$$

$$r' = r'_{\mathbf{m}} + t_{\mathbf{m}}[1 - r'_{\mathrm{SO}} r_{\mathbf{m}}]^{-1} r'_{\mathrm{SO}} t'_{\mathbf{m}}, \tag{20}$$

$$S = \begin{pmatrix} r & t' \\ t & r' \end{pmatrix}. \tag{21}$$

Using these rules we obtain the symmetries of the combined S matrix: $\Sigma_2 t^{\mathrm{T}}(\mathbf{m})\Sigma_2 = t'(-\mathbf{m})$ and $\Sigma_2 r^{\mathrm{T}}(\mathbf{m})\Sigma_2 = r(-\mathbf{m})$ which in turn leads to the Onsager relations. For the two probe configuration, $G(\mathbf{m}) = G(-\mathbf{m})$. For the four probe configuration the transmission probabilities satisfy $T_{ij}(\mathbf{m}) = \mathrm{Tr}(t_{ij} t_{ij}^{\dagger}) = T_{ji}(-\mathbf{m})$. Focusing on the current/voltage configuration: $I_1 = -I_3$, $I_2 = -I_4$, $eV_1 = \mu_3 - \mu_1$ and $eV_2 = \mu_4 - \mu_2$ [31] the relation between currents and voltages can be expressed as [32]:

$$\begin{pmatrix} I_1 \\ I_2 \end{pmatrix} = \begin{pmatrix} \alpha_{11}(\mathbf{m}) & -\alpha_{12}(\mathbf{m}) \\ -\alpha_{21}(\mathbf{m}) & \alpha_{22}(\mathbf{m}) \end{pmatrix} \begin{pmatrix} V_1 \\ V_2 \end{pmatrix}, \tag{22}$$

where the coefficients $\alpha_i j$ can be found in equations (4a)–(4d) of [32]. The Onsager relations can then be expressed as:

$$\alpha_{ij}(\mathbf{m}) = \alpha_{ji}(-\mathbf{m}). \tag{23}$$

If we choose (say) I_1 equal to zero, the relation between the applied current and the spin-Hall voltage is: $I_2 = V_1(\alpha_{11}\alpha_{22} - \alpha_{12}\alpha_{21})/\alpha_{12}$. For phase incoherent conductors, we can ignore the interference terms that arise while obtaining the transmission probabilities, but the Onsager relations equation (23) are unaffected.

This analysis implies the equivalence of two Hall measurements: (i) setting $I_1 = 0$ and measuring V_1 generated by an applied I_2 (figure 1(a)) and (ii) switching magnetization direction, setting $I_2 = 0$ and measuring V_2 (figure 1(b)) generated by an applied I_1. In the next subsection, we shall exploit this symmetry to gain insight into the boundary conditions for a R2DEG|2DEG interface.

3.2. Four-probe set-up and boundary conditions

We now use the Onsager relations from the previous subsection to better understand the spin boundary value problem. Consider the four-probe set-up in figure 1. When the ferromagnetic lead is a Hall contact, the vanishing spin transfer derived by [26] for a (infinitely) wide contact seems to imply that there is neither spin accumulation nor spin current near the ferromagnetic reservoir and therefore no Hall voltage. On the other hand, in the Onsager equivalent measurement, spins are injected from the ferromagnet into the normal region. Since in this case the current is perpendicular to the boundary, the spin accumulations can be matched [26] and a spin accumulation in the SO region exists. However, the diffusion equation (9) implies that a spin accumulation gives rise to a voltage drop in the SO region [18, 35]. Onsager's relations discussed in the previous section imply that these two voltages must be the same provided the injected currents are the same. Thus the result for an infinite contact that a CISA cannot enter Hall contacts [26] appears to be misleading. In the following, we shall demonstrate that the spin accumulations around the Hall contact must be close up to a numerical factor.

We now focus on the current–voltage set-up in figure 1(b). In this case the current is perpendicular to the boundary, so the spin accumulations are continuous across an ideal R2DEG|2DEG interface. Assuming a diffusive ferromagnet magnetized parallel to the current direction and ignoring the resistivity of the normal region, we obtain the spin current polarized in the magnetization direction entering the R2DEG:

$$I_{\mathrm{s}}^{m} \propto \frac{I}{L_{\mathrm{s}}}\frac{\delta D}{\Lambda}, \tag{24}$$

where $L_{\mathrm{s}} = \sqrt{D\tau_{\mathrm{s}}}$ is the (Dyakonov–Perel) spin relaxation length in the R2DEG and

$$\Lambda\,(\mathbf{m}) = L_{\mathrm{s}}^{-1} D \nu_{\mathrm{R}} \mathbf{m}\cdot\boldsymbol{\mu} + L_{\mathrm{sF}}^{-1} D_{\mathrm{F}} \nu_{\mathrm{F}} (1 - \delta D^2/4). \tag{25}$$

Here, L_{sF}, D_{F}, ν_{F} are the spin relaxation length, diffusion constant and average density of states in the ferromagnet, respectively, $\delta D = (\nu_+ D_+ - \nu_- D_-)/(\nu_{\mathrm{F}} D_{\mathrm{F}})$, $\nu_\pm$ and $D_\pm$ are the density of states and diffusion constants of the majority and minority spin electrons, $\boldsymbol{\mu}$ is a linear function of $\mathbf{m}$ of order unity that depends on the details of the geometry of the contact. The spin accumulation in the SO region localized within a depth of L_{s} at the contact aperture acts as a dipole source for the diffusion equation:

$$\nabla^2 n = \boldsymbol{\nabla}\cdot\mathbf{P}, \tag{26}$$

with dipole density $\mathbf{P} = -4K_{\mathrm{s-c}}(\mathbf{z}\times\mathbf{s})/D$. We then estimate the potential drop in the Hall direction to be:

$$\phi = \frac{K_{\mathrm{s-c}}}{D}\frac{1}{W}\int \mathrm{d}\mathbf{r}\, s(\mathbf{r}), \tag{27}$$

which is proportional to the integrated spin accumulation

$$\int \mathrm{d}\mathbf{r}\, s(\mathbf{r}) \approx L_{\mathrm{s}} I \frac{\delta D}{\Lambda}. \tag{28}$$

The potential drop is therefore:

$$\phi_b = \frac{\alpha\tau}{L_{\mathrm{s}}}\frac{I}{W}\frac{\delta D}{\Lambda} = \frac{\alpha}{v_{\mathrm{F}}}\frac{\xi}{\sqrt{1+\xi^2}}\frac{I}{W}\frac{\delta D}{\Lambda}, \tag{29}$$

up to a numerical constant.

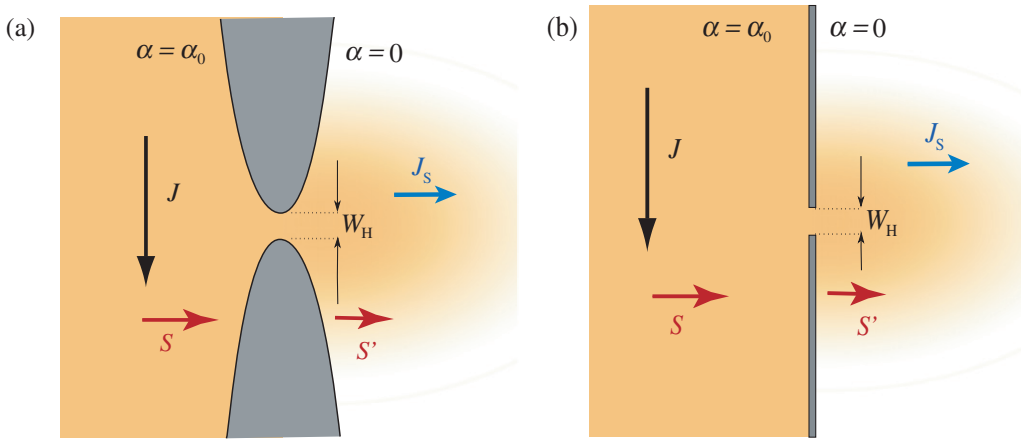

Figure 3. Geometry of the contact: (a) 2DEG with a constriction in the middle. On the left side there is an applied homogeneous current density which is modified near the opening. On the right side, the current density far away from the contact as well as the net charge current flowing from the left region to the right region is zero. However, there is a finite spin current and a finite spin accumulation in the right region. The respective mobilities of the left and right regions are assumed to be the same but the Rashba coefficients are different. (b) An idealized version of (a) used in the calculations of this section. The origin is chosen at the center of the opening with width W_H.

We now focus on the potential drop in the Onsager-equivalent setting in figure 1(a). According to the boundary condition equation (15), CISA does not enter the normal region. Then the potential drop at the ferromagnet–2DEG interface would be zero in contradiction to Onsager's relations. Let us assume that the spin accumulations at the R2DEG and 2DEG near the contact are equal to each other up to a numerical constant Z, i.e. $s_{2DEG} = Z\, s_{R2DEG}$. Then the calculation of the potential drop proceeds similar to [29]. Again ignoring the resistance of the 2DEG region, we obtain a potential drop as:

$$\phi_a = Z \frac{\alpha}{v_F} \frac{\xi}{\sqrt{1+\xi^2}} \frac{I}{W} \frac{\delta D}{\Lambda}, \tag{30}$$

up to a numerical factor. Comparing with equation (29) and noting that we have ignored all numerical factors in the calculations above, we conclude that Z must be a numerical factor of the order of unity in order to satisfy Onsager's relations. In the next section, we shall consider a model for a narrow contact and show that this is indeed the case.

4. Model for spin accumulation near a contact

In this section, we focus on the current density and spin accumulation near a finite contact between a half-infinite R2DEG and a half-infinite 2DEG (figure 3(a)). The model we adopt is sketched in figure 3(b). Asymptotically, we have a constant current density in the left region (R2DEG) in the y-direction whereas in the right region (2DEG) the charge current density

vanishes. The two regions are divided by an infinitely thin and high potential barrier, except for an opening (the contact) of size W_H centered at (0, 0).

We note that the solution to this problem closely follows that of an analogous one in magnetostatics [36]. We proceed by epressing the chemical potential n in terms of the (yet undetermined) solution ϕ of the Laplace equation:

$$\begin{aligned} n &= \frac{J_0 y}{\nu D} + \phi(x, y), \quad \text{if } x < 0, \\ n &= -\phi(x, y), \qquad \text{if } x > 0, \end{aligned} \tag{31}$$

where J_0 is the bulk current density in the R2DEG. The asymmetric behaviour of ϕ in left and right regions is dictated by the current continuity at $x = 0$. The boundary conditions are:

$$\begin{aligned} \phi(0, y) &= -\frac{J_0 y}{2\nu D}, \quad \text{if } |y| < W_H/2, \\ \frac{\partial \phi(0, y)}{\partial x} &= 0, \qquad \text{if } |y| > W_H/2. \end{aligned} \tag{32}$$

Next, we expand ϕ in terms of the modes of the Laplace equation:

$$\phi(x, y) = \int_0^\infty \mathrm{d}k\, A(k) \mathrm{e}^{-k|x|} \sin(ky). \tag{33}$$

The solution to the diffusion equation with the above boundary conditions then reduces to that of a dual integral equation:

$$\begin{aligned} \int_0^\infty \mathrm{d}k\, A(k) \sin(ky) &= -\frac{J_0 y}{2\nu D}, \quad \text{if } |y| < W_H/2, \\ \int_0^\infty \mathrm{d}k\, kA(k) \sin(ky) &= 0, \qquad \text{if } |y| > W_H/2. \end{aligned} \tag{34}$$

Such integral equations arise commonly in potential theory for mixed boundary conditions (see [36] for the solution in 3D). In our case the solution is

$$A(k) = -\frac{j_0 W_H}{4\nu D} \frac{J_1(kW_H/2)}{k}, \tag{35}$$

where J_1 is the Bessel function of the first kind. We may now express the spin accumulations in terms of $A(k)$. For the sake of simplicity, we at first disregard the precession term, proportional to K_p, in the spin diffusion equations (9)–(11). We shall be particularly interested in the question of whether CISA in the SO coupled region can leak out of the contact, into the normal (i.e. no SO interaction) region. In the bulk of the R2DEG, the current is in the y-direction, so the CISA is polarized in the x-direction. Then the general solution to the spin diffusion equations in the R2DEG region is given by:

$$s_x(x, y)^- = \frac{\alpha\tau}{2} \left(\frac{J_0}{\nu D} + \frac{\partial \phi(x, y)}{\partial y} \right) + \delta s_x(x, y), \tag{36}$$

where δs_x satisfies the source-free (i.e. zero charge current) diffusion equation that can be expanded as:

$$\delta s_x(x, y) = \int_0^\infty \mathrm{d}k\, B(k) \mathrm{e}^{-\kappa|x|} \cos(ky), \tag{37}$$

where $\kappa = \sqrt{k^2 + L_s^{-2}}$. For the 2DEG side ($x > 0$), a similar expansion gives:

$$s_x^+(x, y) = \int_0^\infty \mathrm{d}k\, D(k) \mathrm{e}^{-k|x|} \cos(ky). \tag{38}$$

Using the boundary conditions that the spin current is continuous and s_x is discontinuous by an amount equal to $(\alpha\tau/2)\mathrm{d}n/\mathrm{d}y$ [26], we find that the accumulation in the 2DEG satisfies:

$$D(k) = -\frac{\alpha\tau}{2} kA(k) - (\kappa/k)B(k), \tag{39}$$

and $D(k)$ is determined from $A(k)$, through the following dual integral equations:

$$\int_0^\infty \mathrm{d}q\, D(q) \left(1 + \frac{q}{\sqrt{q^2 + \lambda^2}}\right) \cos(q\bar{y}) = -\int_0^\infty \mathrm{d}q\, A(q) \frac{W_\mathrm{H}\alpha\tau q^2}{\sqrt{q^2 + \lambda^2}} \cos(q\bar{y}), \tag{40}$$

if $|\bar{y}| < 1$, and

$$\int_0^\infty \mathrm{d}q\, qD(q) \cos(q\bar{y}) = 0 \tag{41}$$

if $|\bar{y}| > 1$. Here, we have introduced dimensionless variables $q = kW_\mathrm{H}/2$, $\bar{y} = 2y/W_\mathrm{H}$ and $\lambda = W_\mathrm{H}/2L_s$. In the limit $\lambda \gg 1$ (wide contact), expanding equation (40) to leading order in λ^{-1} we obtain that $D(k)$ vanishes like λ^{-1}, in agreement with [26]. In the opposite limit $\lambda \ll 1$ (narrow contact), we again expand equation (40), this time to leading order in λ. We then identify the resulting integral equation with the y derivative of equation (34) times $\alpha\tau/2$. Thus, we show that $D(k) = -\frac{\alpha\tau}{2} kA(k)/2$ solves equation (40) up to order λ^2 corrections. Then the spin accumulation in the 2DEG near a narrow contact is given by:

$$s_x^+(0, y) \approx \frac{\alpha\tau}{4} \frac{\mathrm{d}n(0, y)}{\mathrm{d}y} = \frac{\alpha\tau J_0}{8\nu D}. \tag{42}$$

We see that the spin accumulation in the 2DEG does not vanish even when the mobilities of both sides are equal. For comparison, we also calculate the spin accumulation under the assumption that there is no jump in the accumulations. We obtain that in this case the spin accumulation is twice as large as $s_x^+(0, y)$. The presence of the term proportional to K_p generates z-polarized spin currents going into the 2DEG, owing to the precession of y-polarized spin accumulation as it diffuses out of the R2DEG, but does not change the general picture presented above. We conclude that the choice of the boundary condition for spin accumulation near a narrow contact is not important qualitatively, because either boundary condition produces an identical result up to a numerical factor, in agreement with the Onsager's relations.

5. Numerical results

In this section, we shall provide a numerical demonstration of the results of the previous section, i.e. the possibility of extracting spin accumulations to a normal region with small contacts. We focus on the discretized version of the Hamiltonian (1). Discretization with lattice spacing a yields the following tight-binding representation of $\mathcal{H}_0$ [37]:

$$\mathcal{H}_0 = \frac{\hbar^2}{2ma^2} \Bigg\{ \sum_{n,m} (4 + \bar{U}) c_{n,m}^\dagger c_{n,m} + \sum_{n,m} \Bigg(\Big[-c_{n,m}^\dagger c_{n+1,m} - c_{n,m}^\dagger c_{n,m+1} + \mathrm{i}\bar{\alpha} c_{n,m}^\dagger \sigma_y c_{n+1,m} - \mathrm{i}\bar{\alpha} c_{n,m}^\dagger \sigma_x c_{n,m+1} \Big] + \mathrm{h.c.} \Bigg) \Bigg\}, \tag{43}$$

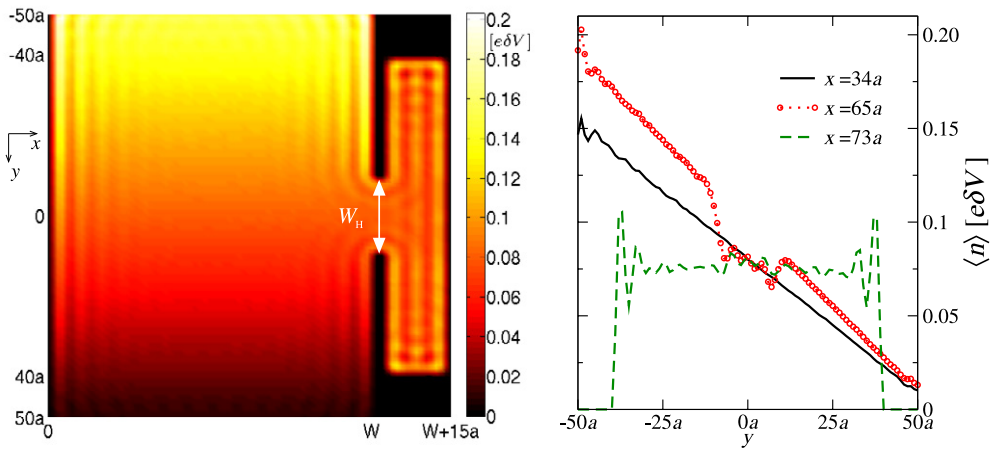

Figure 4. Left panel: geometry used for numerical calculations. A disordered wire with SO coupling and width W connected to two clean leads with SO coupling and to a disordered side-pocket of size $14a \times 80a$ without SO coupling. The colour plot shows the nonequilibrium density $\langle n \rangle$ averaged over 60 000 disorder configurations for a system with $L_{\mathrm{SO}} = 35a$, $W = 68a$ and $W_{\mathrm{H}} = 20a$. The rapid oscillations are due to the finite number of channels in the wire. Nevertheless, the slow varying part satisfies the diffusion equation. Right panel: electron density $\langle n \rangle$ of the system shown in the left panel as a function of vertical coordinate y for fixed horizontal coordinate $x = 34a$ (black solid line), $x = 65a$ (red circles) and $x = 73a$ (green dashed line).

where $n(m)$ is the $x(y)$-coordinate of the site (n, m), $\bar{\alpha} = (ma/\hbar)\alpha$. The abbreviation $c^{\dagger}_{n,m} = (c^{\dagger}_{n,m,+}, c^{\dagger}_{n,m,-})$ was used, where $c^{\dagger}_{n,m,\sigma}$ ($c_{n,m,\sigma}$) creates (annihilates) an electron at site (n, m) with spin orientation σ with respect to the $\hat{z}$-direction. We also define the spin precession length $L_{\mathrm{SO}} = \pi a/\bar{\alpha}$, which is related to L_{s} by $L_{\mathrm{SO}} = 2\pi L_{\mathrm{s}}$ in the dirty limit, but remains well-defined for ballistic systems where there is no spin relaxation. In this model, instead of dilute localized scatterers, we shall assume Anderson disorder: the dimensionless onsite potential $\bar{U}$ is set to a different random value $\bar{U} \in [-U_0/2; U_0/2]$ at each lattice site (n, m) of the disordered region, where U_0 accounts for the strength of the disorder [38]. The parameter U_0 is related to the momentum relaxation rate τ and the electron mean free path $l = v_{\mathrm{F}}\tau$ by:

$$\tau = 48a^2 \frac{m}{\hbar U_0^2}, \qquad l = 48a \frac{\sqrt{\epsilon_{\mathrm{F}}}}{U_0^2}, \tag{44}$$

where $\epsilon_{\mathrm{F}} = (\hbar^2/2m^*a^2)^{-1}E_{\mathrm{F}}$ and E_{F} is the Fermi energy. In the rest of this section, we choose $U_0 = 2$ and $\epsilon_{\mathrm{F}} = 0.38$ in order to ensure that the transport through the system is diffusive. With this choice of parameters the mean free path $l \approx 7.4a$ is smaller than any length scale characterizing the system.

In order to study the spin accumulation extracted to a normal region we focus on the set-up shown in figure 4, where a normal region (i.e. $\bar{\alpha} = 0$) with a size of $80a \times 14a$ is attached to a Rashba SO coupled wire of infinite length, width W and constant finite SO coupling $\bar{\alpha} > 0$ via a contact of size W_{H}. Disorder of strength U_0 is present inside the normal region and in the

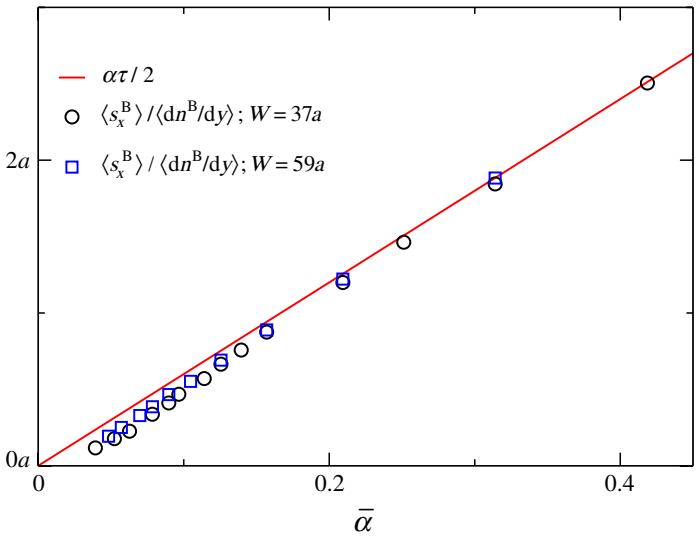

Figure 5. The ratio $\langle s_x^{\mathrm{B}}\rangle/\langle \mathrm{d}n^{\mathrm{B}}/\mathrm{d}x\rangle$ as a function of $\bar{\alpha}$ calculated numerically for two different geometries with $W_{\mathrm{H}} = 20a$ and $W = 37a$ (black dots), $W = 59a$ (blue squares) and estimated as in equation (11) (red line). $\langle s_x^{\mathrm{B}}\rangle$ and $\langle \mathrm{d}n^{\mathrm{B}}/\mathrm{d}x\rangle$ have been evaluated by averaging over 20 000 disorder configurations as well as over the area indicated by the blue square shown in the bottom panel of figure 6.

SO region for $-50a < y < 50a$. We shall use the nonequilibrium Green function method [39] to calculate the lesser Green function $G^<(\vec{r};\vec{r}')$ which is related to spin accumulation according to

$$s_x(\vec{r}) = -\tfrac{1}{2}\mathrm{i}\,\mathrm{Tr}[\sigma_x G^<(\vec{r};\vec{r})] \tag{45}$$

and to the electron density through

$$n(\vec{r}) = -\mathrm{i}\,\mathrm{Tr}[G^<(\vec{r};\vec{r})]. \tag{46}$$

Here, we focus on the ensemble averaged accumulations $\langle s_x\rangle$ and $\langle n\rangle$. The variances are also of interest [40, 41], but we shall not consider them here.

We apply a small bias δV between the chemical potentials of the top and the bottom lead and generate a current in y-direction. The left panel of figure 4 shows the electron density $\langle n\rangle$ inside the system when a current is passed from the top to the bottom. Due to the disorder in the central region ($-50a < y < 50a$) the electron density decreases from top to bottom. In the right panel of figure 4, we show the dependence of $\langle n\rangle$ on y for three different values of x. We observe that $\langle n\rangle$ decreases linearly in the bulk of the SO region (solid line), showing that the system is diffusive. For $x = 65a$ (circles) the side contact at $x = 68a$ disturbs the homogeneous current flow. Inside the normal region, $x = 73a$, $\langle n\rangle$ is approximately constant (dashed line).

The current driven by δV, generates a spin accumulation in the bulk of the R2DEG. According to equation (10), $\langle s_x^{\mathrm{B}}\rangle = (\alpha\tau/2)(\langle \mathrm{d}n^{\mathrm{B}}/\mathrm{d}y\rangle)$ in the bulk. Our simulations agree well with the diffusive result as shown in figure 5 for large enough $\bar{\alpha}$. For smaller values of $\bar{\alpha}$, L_{SO} becomes comparable to the overall length of the disorder region $L = 100a$. In this regime ballistic processes can no longer be neglected, causing slight deviations from the diffusive theory.

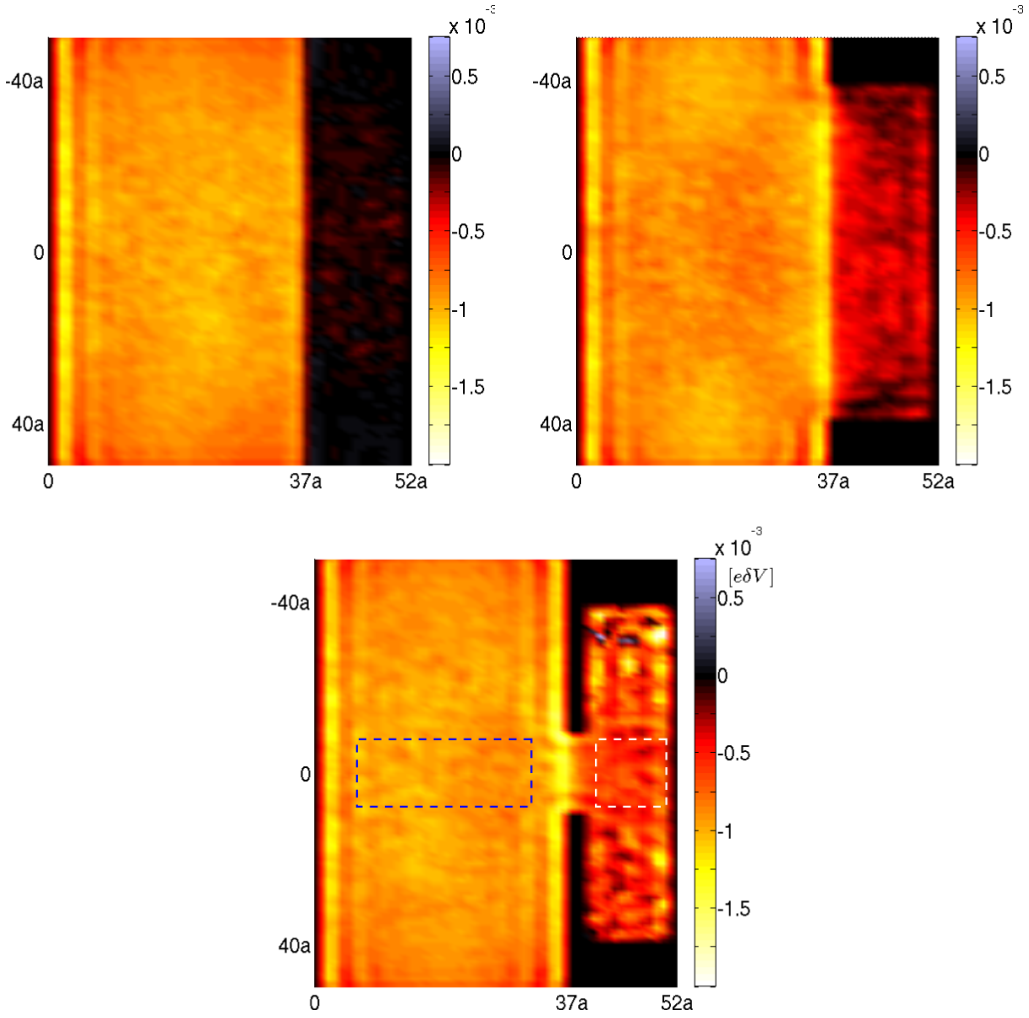

Figure 6. Top left panel: spin accumulation $\langle s_x \rangle$ in a quantum wire of width $W = 52a$ with an abrupt drop of the SO coupling strength at $x = 37a$ from the constant $\bar{\alpha} = \pi/25(L_{\mathrm{SO}} = 25a)$ for $x < 37a$ to zero on the other side. Top right panel: spin accumulation $\langle s_x \rangle$ for a system as shown in figure 4 with $W = 37a$, $W_{\mathrm{H}} = 80a$ and $L_{\mathrm{SO}} = 25a$. Bottom panel: same as top right panel with $W_{\mathrm{H}} = 20a$. In all three panels, $\langle s_x \rangle$ is obtained by averaging over 50 000 disorder configurations.

Having demonstrated that our numerical system is diffusive, we now focus on the spin accumulation in the normal region. In the geometry we have adopted (i.e. a side pocket rather than a side lead), based on the diffusion equations, we expect only CISA (as opposed to spin Hall accumulation) to be present in the normal region. Therefore, below we focus on the x component of the spin accumulation. In figure 6, we show the spin density $\langle s_x \rangle$ averaged over 50 000 impurity configurations inside three distinct systems with $L_{\mathrm{SO}} = 25a$. We note that in agreement with [26], when the interface between R2DEG and 2DEG is infinite (top left panel), the spin accumulation in the 2DEG is much smaller than the bulk spin accumulation. Nevertheless, when the size of the contact is made smaller (top right panel), we observe that the spin accumulation

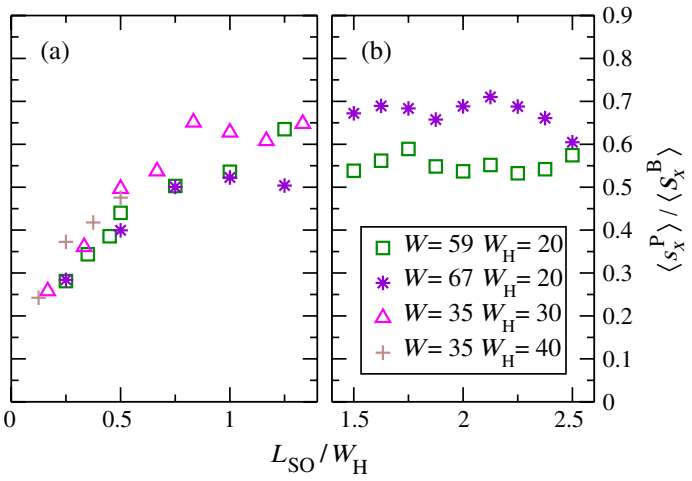

Figure 7. Left panel: average spin accumulation inside the normal region $\langle s_x^{\mathrm{P}}\rangle$ relative to the accumulation in the bulk of the SO region $\langle s_x^{\mathrm{B}}\rangle$ for various geometries averaged over 20 000 disorder configurations as a function of $L_{\mathrm{SO}}/W_{\mathrm{H}}$. Right panel: $\langle s_x^{\mathrm{P}}\rangle/\langle s_x^{\mathrm{B}}\rangle$ for two different geometries averaged over 60 000 disorder configurations.

inside the normal region increases, reaching a comparable value to the spin accumulation in the bulk when the size of the opening is comparable to L_{SO} (bottom panel). In order to demonstrate this further, we evaluate $\langle s_x^{\mathrm{B}}\rangle$ by averaging the spin accumulation in the bulk over the blue square shown in figure 6 and $\langle s_x^{\mathrm{P}}\rangle$ by averaging the spin accumulation in the normal conducting side-pocket over the white square shown in figure 6. In figure 7, we plot the ratio $\langle s_x^{\mathrm{P}}\rangle/\langle s_x^{\mathrm{B}}\rangle$ as a function of $L_{\mathrm{SO}}/W_{\mathrm{H}}$, for various values of system and contact sizes. We observe that starting from small $L_{\mathrm{SO}}/W_{\mathrm{H}}$, the spin accumulation increases with $L_{\mathrm{SO}}/W_{\mathrm{H}}$, approaching to $\approx$0.5–0.7. This value is in between the estimates 0.5 and 1.0 based on diffusion equations using the boundary conditions (15) and (14), respectively. For small values of $L_{\mathrm{SO}}/W_{\mathrm{H}}$ (figure 7, left panel), $\langle s_x^{\mathrm{P}}\rangle/\langle s_x^{\mathrm{B}}\rangle$ is of order $(L_{\mathrm{SO}}/W_{\mathrm{H}})$ in agreement with the analytical calculation above. We note, however, that in this limit the system we considered is close to the clean limit $L_{\mathrm{SO}} \sim l$, where deviations from the diffusion equations might be expected. Currently, we are working on larger systems in order to explore small $L_{\mathrm{SO}}/W_{\mathrm{H}}$ in the dirty limit [42].

6. Conclusions

In this work, we considered the problem of extracting current-induced spins generated in a region with SO coupling into a region with vanishing (or small) SO coupling, where the spin relaxation time is long. To this end, we focused on the spin boundary conditions between a SO coupled region and a normal region. Although for an infinite interface the spins are confined to the SO region via the boundary SHE, we have shown by solving a model problem as well as doing numerical simulations that for a finite interface the spin accumulations generated in the SO region can be extracted to a normal region. The amount of extracted spin accumulation is equal to that of the SO region up to a geometrical factor of the order of unity.

Acknowledgments

We profited from discussions with Y Tserkovnyak. IA and GEWB would like to thank A Brataas and Y Tserkovnyak for making a preprint of [27] available to them. IA and KR acknowledge support through the Deutsche Forschungsgemeinschaft within the cooperative research center SFB 689 'Spin phenomena in reduced dimensions'. MS acknowledges support through the Studienstiftung des Deutschen Volkes. MW acknowledges support through the Deutsche Forschungsgemeinschaft within GRK638. GEWB has been supported by the FOM, NanoNed, and EC Contract IST-033749 'DynaMax'.

References

[1] Zutić I, Fabian J and Das Sarma S 2004 *Rev. Mod. Phys.* **76** 323
[2] Vas'ko F T and Prima N A 1979 *Sov. Phys. Solid State* **21** 994
Levitov L S, Nazarov Yu V and Eliashberg G M 1985 *Zh. Eksp. Teor. Fiz.* **88** 229
[3] Aronov A G and Lyanda-Geller Yu B 1989 *JETP Lett.* **50** 431
[4] Edelstein V M 1990 *Solid State Commun.* **73** 233
Inoue J I, Bauer G E W and Molenkamp L W 2003 *Phys. Rev.* B **67** 033104
[5] Kato Y K, Myers R C, Gossard A C and Awschalom D D 2004 *Nature* **427** 50
KatoY K, Myers R C, Gossard A C and Awschalom D D 2004 *Phys. Rev. Lett.* **93** 176601
Silov A Yu *et al* 2004 *Appl. Phys. Lett.* **85** 5929
Ganichev S D, Danilov S N, Schneider P, Bel'kov V V, Golub L E, Wegscheider W, Weiss D and Prettl W 2004 *Preprint* cond-mat/0403641
Ganichev S D, Danilov S N, Schneider P, Bel'kov V V, Golub L E, Wegscheider W, Weiss D and Prettl W 2006 *J. Magn. Magn. Mater.* **300** 127
[6] Dyakonov M I and Perel V I 1971 *Sov. Phys.—JETP Lett.* **13** 467
Dyakonov M I and Perel V I 1971 *Phys. Lett.* A **35** 459
[7] Hirsch J E 1999 *Phys. Rev. Lett.* **83** 1834
[8] Zhang S 2000 *Phys. Rev. Lett.* **85** 393
Shchelushkin R V and Brataas A 2005 *Phys. Rev.* B **71** 045123
Hu J *et al* 2003 *Int. J. Mod. Phys.* B **17** 5991
Shen S-Q 2004 *Phys. Rev.* B **70** 081311
Culcer D *et al* 2004 *Phys. Rev. Lett.* **93** 046602
Sinitsyn N A *et al* 2004 *Phys. Rev.* B **70** 081312
Burkov A A *et al* 2004 *Phys. Rev.* B **70** 155308
[9] Sinova J *et al* 2004 *Phys. Rev. Lett.* **92** 126603
[10] Murakami S, Nagaosa N and Zhang S-C 2003 *Science* **301** 1348
Murakami S, Nagaosa N and Zhang S-C 2004 *Phys. Rev.* B **69** 235206
[11] Inoue J-I, Bauer G E W and Molenkamp L W 2004 *Phys. Rev.* B **70** 041303
[12] Mishchenko E G, Shytov A V and Halperin B I 2004 *Phys. Rev. Lett.* **93** 226602
[13] Burkov A A, Núñez A S and MacDonald A H 2004 *Phys. Rev.* B **70** 155308
[14] Sinova J, Murakami S, Shen S-Q and Choi M-S 2006 *Solid State Commun.* **138** 214
[15] Adagideli İ and Bauer G E W 2005 *Phys. Rev. Lett.* **95** 256602
[16] Kato Y K, Myers R C, Gossard A C and Awschalom D D 2004 *Science* **306** 1910
Sih V, Myers R C, Kato Y K, Lau W H, Gossard A C and Awschalom D D 2005 *Nat. Phys.* **1** 31–5
[17] Wunderlich J, Kästner B, Sinova J and Jungwirth T 2005 *Phys. Rev. Lett.* **94** 047204

[18] Saitoh E, Ueda M, Miyajima H and Tatara G 2006 *Appl. Phys. Lett.* **88** 182509
Valenzuela S O and Tinkham M 2006 *Nature* **442** 176
Kimura T, Otani Y, Sato T, Takahashi S and Maekawa S 2007 *Phys. Rev. Lett.* **98** 156601
Kimura T, Otani Y, Sato T, Takahashi S and Maekawa S 2007 *Phys. Rev. Lett.* **98** 249901
[19] Schliemann J and Loss D 2005 *Phys. Rev.* B **71** 085308
[20] Raimondi R and Schwab P 2005 *Phys. Rev.* B **71** 033311
[21] Mal'shukov A G, Wang L Y, Chu C S and Chao K A 2005 *Phys. Rev. Lett.* **95** 146601
[22] Rashba E I 2006 *Physica* E **34** 31
[23] Galitski V M, Burkov A A and Das Sarma S 2006 *Phys. Rev.* B **74** 115331
[24] Bleibaum O 2006 *Phys. Rev.* B **73** 035322
Bleibaum O 2006 *Phys. Rev.* B **74** 113309
[25] Raimondi R, Gorini C, Schwab P and Dzierzawa M 2006 *Phys. Rev.* B **74** 035340
[26] Tserkovnyak Y, Halperin B I, Kovalev A A and Brataas A 2007 *Phys. Rev.* B **76** 085319
[27] Brataas A, Mal'shukov A G and Tserkovnyak Y 2007 *New J. Phys.* **9** 345
[28] Mathur H and Stone A D 1992 *Phys. Rev. Lett.* **68** 2964
[29] Adagideli I, Bauer G E W and Halperin B I 2006 *Phys. Rev. Lett.* **97** 256601
[30] Onsager L 1931 *Phys. Rev.* B **38** 2265
[31] Casimir H B G 1945 *Rev. Mod. Phys.* **17** 343
[32] Büttiker M 1986 *Phys. Rev. Lett.* **57** 1761
[33] Hankiewicz E M *et al* 2005 *Phys. Rev.* B **72** 155305
[34] Beenakker C W J 1997 *Rev. Mod. Phys.* **69** 731
[35] Ganichev S D, Ivchenko E L, Bel'kov V V, Tarasenko S A, Sollinger M, Weiss D, Wegscheider W and Prettl W 2002 *Nature* **417** 153
[36] Jackson J D 1975 *Classical Electrodynamics* 2nd edn (New York: Wiley) section 5.13
[37] Nikolić B K, Zârbo L P and Souma S 2005 *Phys. Rev.* B **72** 75361
Hankiewicz E M, Molenkamp L W, Jungwirth T and Sinova J 2004 *Phys. Rev.* B **70** 241301
Sheng L, Sheng D N and Ting C S 2005 *Phys. Rev. Lett.* **94** 016602
[38] Kramer B and MacKinnon A 1993 *Rep. Prog. Phys.* **56** 1469
[39] Rammer J and Smith H 1986 *Rev. Mod. Phys.* **58** 323
[40] Ren W, Qiao Z, Wang J, Sun Q and Guo H 2006 *Phys. Rev. Lett.* **97** 066603
[41] Bardarson J, Adagideli I and Jacquod Ph 2007 *Phys. Rev. Lett.* **98** 196601
[42] Scheid M and Adagideli I, unpublished